RF Wave and Energy Propagation in High Field MRI

C. M. Collins[1], C. Kao[1], and A. G. Webb[2]
[1]PSU College of Medicine, Hershey, PA, United States, [2]Leiden University Medical Center, Leiden, Netherlands

Introduction: As wavelength effects have become a factor in MRI at high fields, a variety of approaches to characterize wave behavior in MRI have been used (1-5). All of these methods can be seen as describing waves of RF energy that propagate into the sample. Depending upon the sample properties and the number, placement, geometry, and orientation of the sources, these waves can interfere in different ways to form a variety of patterns in the magnitude of the pertinent circularly-polarized magnetic fields.

In whole-body images at 7T it has been observed that fields can propagate further from the coil than typically observed at lower field strengths (6). Recently, the observation that the magnet bore can act as a waveguide at frequencies of 300MHz and above has led to MRI studies with antennas designed to send a circularly-polarized wave down the magnet bore (7-10). These experiments have produced very intriguing results and a fair amount of interest. Here we use numerical simulations to explore the basic nature of RF wave and energy propagation in MRI of the human head at 7T using either a body-sized TEM array or patch antenna remote from the subject to achieve excitation.

Methods: Models of the human body (11) in a 3m long, 60cm diameter cylindrical RF shield was created for use with the Finite-Difference Time-Domain (FDTD) method. Simulations were performed alternately with a body-sized TEM array (6) located about the head and driven as with a mode 1 resonance in quadrature, or with a large circularly-polarized patch antenna (5) placed at the end of the cylinder (Fig. 1). The simulation was run at 300 MHz using commercially-available software (xFDTD, Remcom Inc.). Complex electric and magnetic fields were recorded and the results were processed in Matlab (The Mathworks) to produce animated plots of the RF magnetic (B_1) field magnitude through time, the time-average Poynting vector ($\mathbf{S}_{ave}$, an indication of the direction and strength of energy propagation), and the magnitude of the circularly-polarized component of the B_1 field pertinent to nuclear excitation (B_1^+).

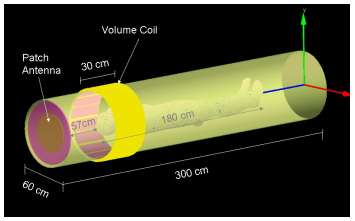

Figure 1. Model used for Numerical simulations.

Results and Discussion: Figure 2 shows the distribution of B_1^+ and $\mathbf{S}_{ave}$ on the sagittal plane passing through the middle of the body as produced with the TEM array and with the patch antenna. Although the direction of energy propagation ($\mathbf{S}_{ave}$) towards the head from the source is largely in the axial direction for the patch antenna and largely in the radial direction for the TEM array, within the body the direction is mainly perpendicular to the surface of the body for either source. A left-right component to $\mathbf{S}_{ave}$ observed between the patch antenna and the body may be due to interference between incident and reflected waves in this region. Also, the TEM array is seen to produce RF energy travelling down the bore at locations remote from the coil in either direction. Animated plots of B_1 field magnitude through time show shorter waves traveling at a slower speed within the body than in the surrounding air, and significant change in direction at the surface of the body, consistent with $\mathbf{S}_{ave}$, and with concepts related to refraction. Similar effects are also seen in simulations for a small loop coil near the leg (12).

It is well known that the location, orientation, and drive of the RF source or sources in MRI can have a dramatic effect on the distribution of B_1^+ and it is obvious that the location of the source also affects the direction of field and energy propagation from the source to the sample. However, no matter what the source, at 300 MHz in a whole-body system the direction of propagation within the body is primarily perpendicular to the surface of the body, while remote from the source and outside of the body, is largely parallel to the bore axis. If the B_1^+ distribution within the body is thought of as a result of superimposed waves entering at the surface of the body (4, 5), it is clear that the B_1^+ distribution is a result of the relative magnitudes and phases of the fields at the surface, and thus depends strongly on the placement, orientation, and drive of the sources. Thus, there is much to be gained from exploring very different approaches. For example, whereas the TEM array placed about the head produces a strong field near its center, where interference is most constructive, the patch antenna produces relatively strong B_1^+ fields in regions of narrow or sparse conductive tissue (neck, arms, and legs), where waves at the surface can penetrate to interfere constructively before significant attenuation occurs. In all cases the field strength generally decreases with distance from the coil.

While this work is dedicated to exploring the basic nature of wave and energy propagation from very different RF sources in high field MRI – the patch antenna and TEM array - in other works we attempt quantitative examination of the relative benefits (homogeneity and SAR) of these sources used separately and simultaneously.

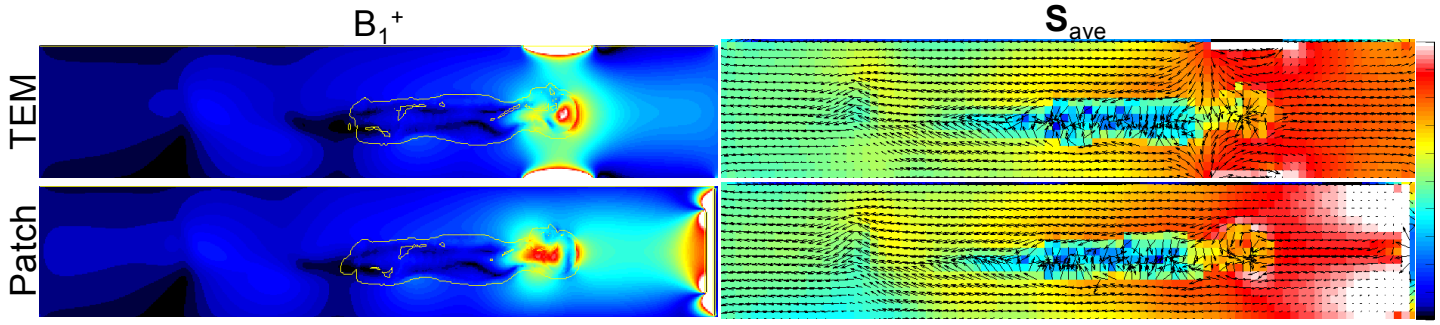

Figure 2. Distributions of B_1^+ and $\mathbf{S}_{ave}$ on the mid-sagittal plane for excitation with a body-sized TEM resonator about the head and a patch antenna located near the end of the magnet bore. For B_1^+ the color scale (far right) ranges from 0 to 10μT. Yellow contours in B_1^+ plot indicate boundaries between conductive materials and air. For $\mathbf{S}_{ave}$, arrows indicating direction of propagation are all the same length in three dimensions, so shorter in-plane projections have a significant through-plane component. The color scale for $\mathbf{S}_{ave}$ ranges from 0 to 10 and indicates $\mathrm{Log}[|\mathbf{S}_{ave}|/\max(|\mathbf{S}_{ave}|)]$. All values are for 1kW input power.

References: 1. Foo *et al*., MRM 1992;23:287-301
2. Tofts, JMRb 2004;104:143-7
3. Yang *et al*., MRM 2002;47:982-9
4. Collins *et al*., JMRI 2005;21:192-6
5. Moortele et al., MRM 2005;54:1503
6. Vaughan *et al*., MRM 2009;61:244-8
7. Brenner *et al*., Nature 2009;457:994-9
8. van den Berg *et al*., '08 ISMRM p. 2944
9. Wiggins *et al*., 2009 ISMRM p. 2942
10. Smith *et al*., 2008 ISMRM p. 2941
11. Christ *et al*., 2007 ICEBEA, S-4-2
12. Webb *et al*., MRM *in press*

Acknowledgement: Support was provided by the NIH through R01EB000454 and R01EB000895 and by the Pennsylvania Department of Health.